Hyperfine Interactions **138:** 289–294, 2001.

Experimental Search for μd ^{3}He Fusion

P. E. KNOWLES[1,*], V. M. BOREIKO[2], V. M. BYSTRITSKY[2], M. FILIPOWICZ[3], O. HUOT[1], F. MULHAUSER[1], V. N. PAVLOV[2], F. M. PENKOV[2], C. PETITJEAN[4], N. P. POPOV[5], V. G. SANDUKOVSKY[2], L. A. SCHALLER[1], H. SCHNEUWLY[1], V. A. STOLUPIN[2] and J. WOŹNIAK[3]

[1] *Université de Fribourg, CH-1700 Fribourg, Switzerland; e-mail: Paul.Knowles@unifr.ch*
[2] *Joint Institute for Nuclear Research, Dubna 141980, Russia*
[3] *Institute of Physics and Nuclear Techniques, 30150 Cracow, Poland*
[4] *Paul Scherrer Institute, CH-5232 Villigen, Switzerland*
[5] *Sektion Physik der Universität München, München, Germany*

Abstract. The vast majority of muon catalyzed fusion research has been concerned with muonic molecules of hydrogen isotopes only, since the dynamics of higher-Z muonic atoms in general preclude the formation of molecular systems. In the specific case of hydrogen–helium mixtures, bound muonic molecular states can exist, and thus it is possible to search for the reaction

$$\mu\mathrm{d}\,{}^3\mathrm{He} \xrightarrow{\tilde{\lambda}_f} \mu + \alpha(3.66\ \mathrm{MeV}) + \mathrm{p}(14.64\ \mathrm{MeV}).$$

Until recently, the theoretical predictions for the nuclear fusion rate in the μd ^{3}He molecule, $\tilde{\lambda}_f$, ranged over one order of magnitude, from 10^5 to 10^6 per second. An experimental upper limit has been measured for $\tilde{\lambda}_f$ in HD + ^{3}He giving a value ($< 6 \times 10^4$ s^{-1} [1]). We report on the analysis of an experiment in D_2 + ^{3}He which has shown a signal coming either from the muon catalyzed reaction, or from the fusion in flight of ^{3}He's formed from dμd fusion.

Key words: muon catalyzed fusion, deuterium, helium–three, muonic molecular formation.

1. Introduction

A search for the muon catalyzed $\mu\mathrm{d} + {}^3\mathrm{He} \rightarrow p + {}^4\mathrm{He} + \mu$ fusion reaction has been carried out in a gaseous mixture of D_2 + ^{3}He. The experiment was performed in the improved version of the apparatus reported in [2].

The kinetics of the reaction are shown in Figure 1, which also establishes the notation used for the rates. The equations represented by the figure decouple easily into a dμd sector and a μd + ^{3}He sector, which makes the analytic solution relatively straightforward (see also [3, 4]).

* Corresponding author.

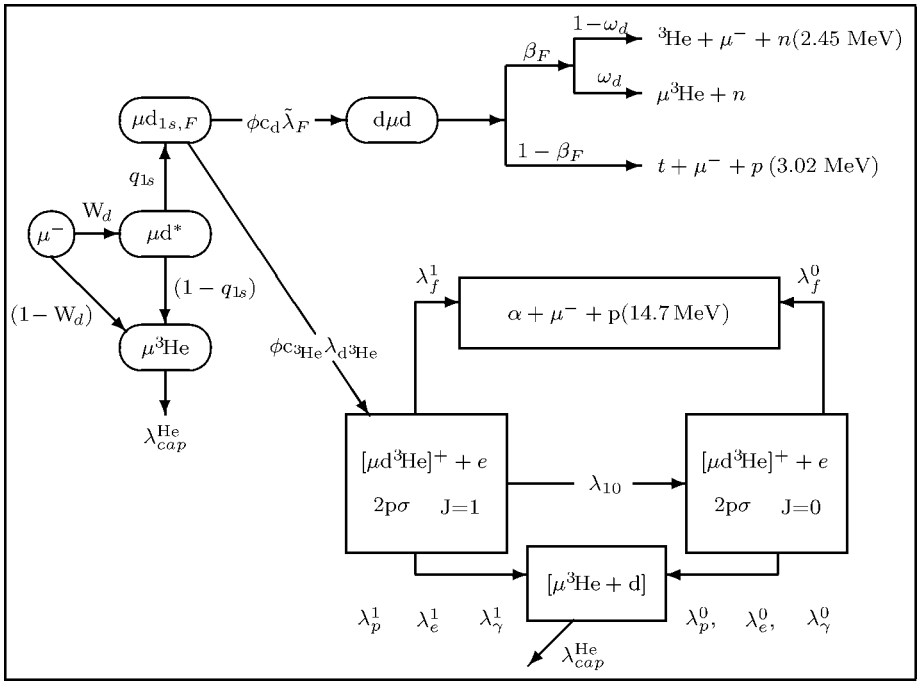

Figure 1. A simplified kinetics of the reactions leading to μd^{3}He fusion in mixtures of D_2 and ^{3}He gases. Muon cycling and decay have not been drawn, and energies quoted are for the detected particle. The hyperfine exchange rates, $\tilde{\lambda}_{FF'}$, between $\mu\mathrm{d}_{\frac{3}{2}}$ and $\mu\mathrm{d}_{\frac{1}{2}}$ states (here denoted $\mu\mathrm{d}_F$) are included in the kinetics equations, but have not been drawn in the figure.

The total fusion proton yield is summed from the spin states of the μd^{3}He:

$$\begin{aligned} Y_p &= \left(\frac{\lambda^1_f}{\lambda_{10} + \lambda_{\Sigma 1}} + \frac{\lambda_{10}}{\lambda_{10} + \lambda_{\Sigma 1}} \frac{\lambda^0_f}{\lambda_{\Sigma 0}} \right) \frac{\phi \mathrm{c}_{^3\mathrm{He}} \lambda_{\mathrm{d}^3\mathrm{He}} N_\mu \mathrm{W}_d q_{1s}}{\lambda_{\mu\mathrm{d}}} \\ &= \left(\frac{\tilde{\lambda}_f}{\lambda_\Sigma} \right) \frac{\phi \mathrm{c}_{^3\mathrm{He}} \lambda_{\mathrm{d}^3\mathrm{He}} N_\mu \mathrm{W}_d q_{1s}}{\lambda_{\mu\mathrm{d}}}, \end{aligned}$$

where the effective fusion rate $\tilde{\lambda}_f$ and effective deexcitation rate are defined by:

$$\begin{aligned} \tilde{\lambda}_f &= \left(\lambda^1_f \frac{\lambda_{\Sigma 0}}{\lambda_{10} + \lambda_{\Sigma 0}} + \lambda^0_f \frac{\lambda_{10}}{\lambda_{10} + \lambda_{\Sigma 0}} \right), \\ \lambda_\Sigma &= \left(\lambda_{\Sigma 1} \frac{\lambda_{\Sigma 0}}{\lambda_{10} + \lambda_{\Sigma 0}} + \lambda_{\Sigma 0} \frac{\lambda_{10}}{\lambda_{10} + \lambda_{\Sigma 0}} \right). \end{aligned}$$

The key to measuring the fusion rate depends on the accurate determination of the proton yield, or, in the case of setting an upper limit on the rate, on the accurate evaluation of the background.

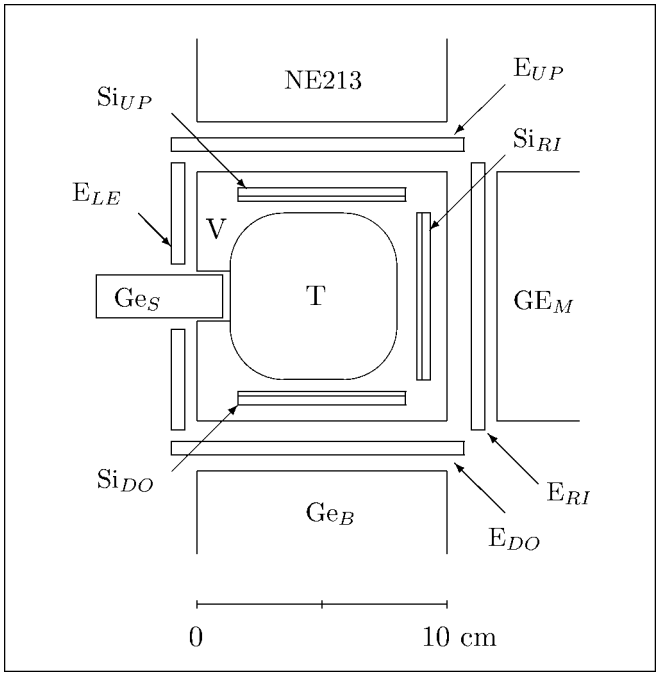

Figure 2. A schematic view of the experimental apparatus as seen by an incoming muon. The cryogenic target gas mixtures were confined to region "T", which was thermally isolated from the containment vessel by the vacuum space "V".

2. Experiment

A schematic view of the apparatus is shown in Figure 2. Of note are the three pair of Si detectors, each pair composed of a thin (300 μm) dE, and a thick (3.6 mm) E detector. This arrangement permits a good identification of protons, deuterons, and electrons based on energy loss behavior. The E_{XX} detectors detect the muon decay electron, important for background suppression. Note also Ge_S, a small germanium detector capable of detecting the 6.8 keV X-ray from the radiative deexcitation channel of the μd^3He molecule.

A mixture with atomic ^{3}He concentration of 0.0496(10) was used under two conditions of temperature and pressure: high pressure (34.5 K, 1222.5 kPa) and low pressure (32.8 K, 512.95 kPa). Based on the equations of state in [5] the corresponding densities relative to LHD (4.25×10^{22} atoms/cm^3) were 0.0585(12) for the low pressure target and 0.168 for the high pressure target. The uncertainty on the high pressure target has not yet been determined due to complications related to systematic uncertainties in the temperature measurement.

Figures 3 and 4 show the energy spectrum seen by the small germanium detector, Ge_S, when the low pressure target was in use. By demanding that the electron detectors see the muon decay electron between (0.1,5.1) μs after the X-ray event

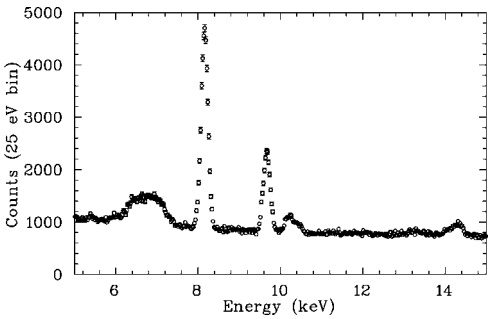

Figure 3. Energy spectrum of the Ge_S detector for the low pressure mixture target. Visible are the helium K_α, K_β, $K_{\rm rest}$, and the 6.8 keV line.

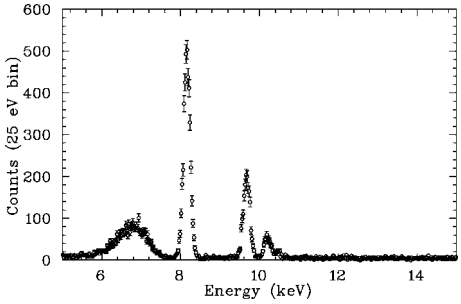

Figure 4. Energy spectrum of the Ge_S detector (Figure 3) with the delayed electron condition applied. The background is clearly very strongly suppressed.

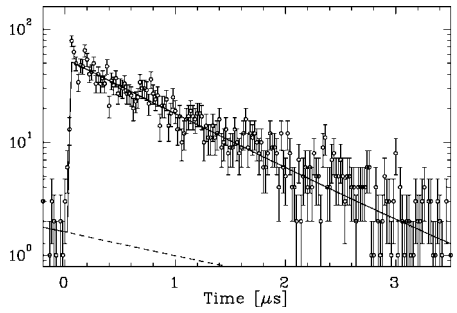

Figure 5. Time spectrum of the 6.8 keV line from the low pressure mixture.

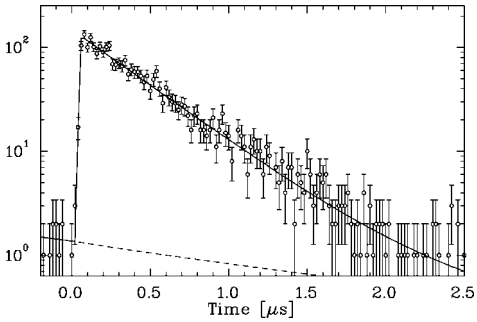

Figure 6. Time spectrum of the 6.8 keV line from the high pressure mixture.

in Figure 3 creates the spectrum in Figure 4, where the background has been very strongly suppressed (the so-called delayed electron condition).

Figures 5 and 6 show the time spectra of the 6.8 keV line including the delayed electron condition. Fits to the spectra are consistent with a single exponential as expected by the kinetics, and result in values for λ_{d^3He} (extracted from the measured $\lambda_{\mu d}$ rate) of $240(13)_{\rm stat}(15)_{\rm sys}$ μs^{-1} for the low pressure mixture and $244(6)_{\rm stat}(16)_{\rm sys}$ μs^{-1} for the high pressure mixture. The systematic uncertainties cover the possible range of background models used in the fits, including the extreme case where the background is set to zero.

Figure 7 shows a density plot of the energy loss in the thin Si detector (dE) versus the total energy of the particle ($E + dE$) for the low pressure mixture target. The classical banding structure shows a good separation of electron, proton, and deuteron events. Figure 8 represents the same data as Figure 7 but now with the delayed electron condition applied. In the region consistent with 14.7 MeV protons there are excess events. By comparing the ratio of events with and without the delayed electron requirement from regions of the plots where there can be no fusion

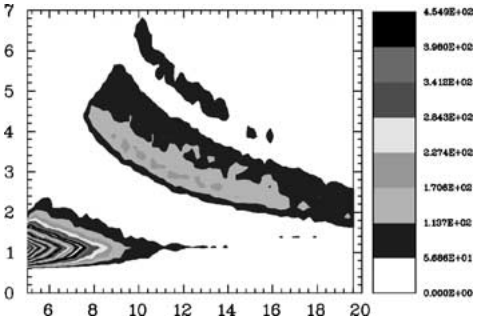

Figure 7. Energy loss versus total energy of particles in the Si detector pairs. The separation of electrons (lower left), protons (main band in center), and deuterons is well accomplished.

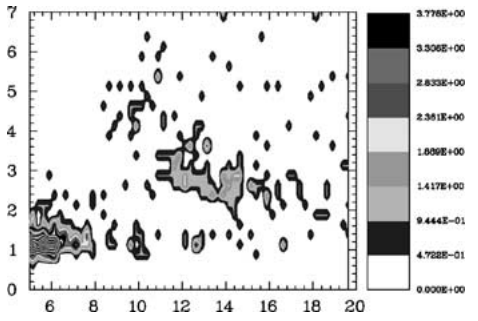

Figure 8. Energy loss versus total energy of particles in the Si detector pairs with the delayed electron condition applied. The excess in number of proton events above the expected background level are clearly visible.

protons it is possible to predict the number of background counts in the region where there are possible fusion events. By that treatment, we have found 34(10) excess events.

The provenance of those events is still not resolved. Unlike Maev *et al.* [1] where HD was used, our experiment used D_2 and hence allowed dμd fusion to occur, creating ^{3}He at 0.82 MeV. This ^{3}He has the possibility to fuse with a deuteron while slowing down, creating the energetic proton for which we are searching. Of course, after the dμd fusion, the muon is available to create a delayed electron and hence mimic exactly the signature of the muon catalyzed event. *If* the events we see are really from μd + ^{3}He fusion, then the rate we can determine for $\tilde{\lambda}_f$ is of the order 0.7 μs^{-1}, an order of magnitude higher than the limit determined in [1], which is a reason to doubt that the events come from the μd + ^{3}He catalyzed reaction.

3. Present status

We have measured the transfer rate for muons from μd to ^{3}He, under two conditions of pressure (and hence density) and found the same result both times. Our preliminary value of $\lambda_{d^3He} = 242(20)\ \mu s^{-1}$, where the error is dominated by systematics, is consistent with the measurement of Maev *et al.* [6], but is in sharp disagreement with the work of Gartner *et al.*, whose value was 185.6(77) μs^{-1} [7]. This difference has not yet been understood.

The d + ^{3}He fusion signal is present, but whether or not it is catalyzed by the muon directly, or is caused only by the ^{3}He from dμd fusion is still under investigation. All present indications are that the signal is from fusion in flight of the ^{3}He's from dμd fusion, but since the analysis is still underway, no final result can be given.

Acknowledgements

The authors wish to thank L. Schellenberg, A. Del Rosso, and C. Donche-Gay for assistance during data taking. This work is supported by the Swiss National Science Foundation, by the Russian Foundation for Basic Research (grant 01-02-16483), and by the Polish Committee for Scientific Research.

References

1. Maev, E. M. *et al.*, *Hyp. Interact.* **118** (1999), 171.
2. Del Rosso, A. *et al.*, *Hyp. Interact.* **118** (1999), 177.
3. Bystritsky, V. M., Czaplinski, W. and Popov, N., *Eur. Phys. J. D* **5** (1999), 185.
4. Bogdanova, L. N., Gershtein, S. S. and Ponomarev, L. I., PSI Preprint 97–33, 1997.
5. Jacobson, R. T., Penoncello, S. G. and Lemmon, E. W., *Thermodynamic Properties of Cryogenic Fluids*, Plenum Press, New York, 1997.
6. Maev, E. M. *et al.*, *Hyp. Interact.* **119** (1999), 121.
7. Gartner, B. *et al.*, *Phys. Rev. A* **62** (2000), 012501.